PROCEEDINGS OF SPIE

SPIEDigitalLibrary.org/conference-proceedings-of-spie

Fabrication, characterisation, and epitaxial optimisation of MOVPE-grown resonant tunnelling diode THz emitters

Razvan Baba
Kristof J. P. Jacobs
Benjamin J. Stevens
Brett A. Harrison
Toshikazu Mukai
Richard A. Hogg

SPIE.

Downloaded From: https://www.spiedigitallibrary.org/conference-proceedings-of-spie on 8/24/2017 Terms of Use: https://spiedigitallibrary.spie.org/ss/TermsOfUse.aspx

Fabrication, Characterisation, and Epitaxial Optimisation of MOVPE-Grown Resonant Tunnelling Diode THz emitters

Razvan Baba *[a], Kristof J.P. Jacobs[b], Benjamin J. Stevens[b], Brett A. Harrison[c], Toshikazu Mukai[d], Richard A. Hogg[a]

[a]School of Engineering, University of Glasgow, Glasgow, G12 8LT, UK,
[b]Dept. of Electronic & Electrical Engineering, Centre for Nanoscience & Technology, University of Sheffield, Sheffield, S3 7HQ, UK

[c]EPSRC National Centre for III-V Technologies, University of Sheffield, Sheffield, S3 7HQ, UK
[d]Rohm Co. Ltd., Ukyo-ku, Kyoto 615-8585, Japan

ABSTRACT

Resonant tunnelling diodes (RTDs) are a strong candidate for future wireless communications in the THz region, offering compact, room-temperature operation with Gb/s transfer rates. We employ the InGaAs/AlAs/InP material system, offering advantages due to high electron mobility, suitable band-offsets, and low resistance contacts. We describe an RTD emitter operating at 353GHz, radiating in this atmospheric transmittance window through a slot antenna. The fabrication scheme uses a dual-pass technique to achieve reproducible, very low resistivity, ohmic contacts, followed by accurate control of the etched device area. The top contact connects the device via the means of an air bridge. We then proceed to model ways to increase the resonator efficiency, in turn improving the radiative efficiency, by changing the epitaxial design. The optimization takes into account the accumulated stress limitations and realities of reactor growth. Due to the absence of useful in-situ monitoring in commercially-scalable metal-organic vapour phase epitaxy (MOVPE), we have developed a robust non-destructive epitaxial characterisation scheme to verify the quality of these mechanically shallow and atomically thin devices. A dummy copy of the active region element is grown to assist with low temperature photoluminescence spectroscopy (LTPL) characterisation. The resulting linewidths limits the number of possible solutions of quantum well (QW) width and depth pairs. In addition, the doping levels can be estimated with a sufficient degree of accuracy by measuring the Moss-Burstein shift of the bulk material. This analysis can then be combined with high resolution X-ray diffractometry (HRXRD) to increase its accuracy.

Keywords: resonant tunnelling diode, terahertz emitter, MOVPE, characterisation

1. INTRODUCTION

Resonant tunnelling diodes (RTDs) are a strong contender to provide solutions for future wireless communications interconnects in the THz region, offering compact, room-temperature operation with bit rates in the order of Gb/s, as demonstrated by Mukai *et al.* [1]. They have been coupled to antennae to realise effective room temperature emitters of THz radiation, capable of 1.92 THz [2]. Other possible applications include sensing and imaging[3], and high resolution radar[4]. Practical devices will require high output powers and better efficiency than competing technologies, as well as temperature-insensitive operation. In addition, applications destined for communications benefit greatly from a compact, chip-sized emitter.

In this work, we describe an RTD emitter operating at 353GHz peak wavelength through a slot antenna, initially demonstrated with a collimating hyperhemispherical Si lens[5]. The fabrication scheme uses a dual-pass technique to achieve reproducible, very low resistivity, ohmic contacts, followed by an accurate control of the etched area device area. The top contact connects the device via the means of an air bridge. We then proceed to model ways to increase the radiative efficiency of such devices, by altering the epitaxial design. The optimization takes into account the accumulated stress limitations. We then conclude by providing a novel structure to assist with low temperature photoluminescence spectroscopy (LTPL) characterisation. This analysis can then be combined with high resolution X-ray diffractometry (HRXRD) to increase its accuracy.

Quantum Sensing and Nano Electronics and Photonics XIV, edited by Manijeh Razeghi,
Proc. of SPIE Vol. 10111, 101113A · © 2017 SPIE · CCC code: 0277-786X/17/$18
doi: 10.1117/12.2252377

Downloaded From: https://www.spiedigitallibrary.org/conference-proceedings-of-spie on 8/24/2017 Terms of Use: https://spiedigitallibrary.spie.org/ss/TermsOfUse.aspx

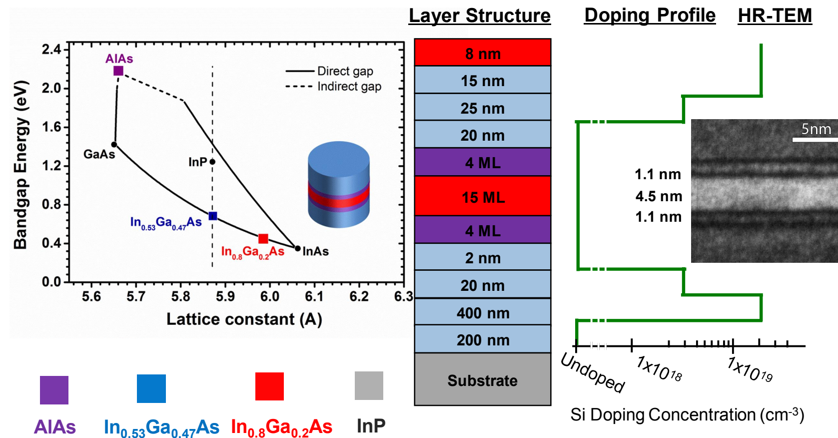

Figure 1. Schematic layer structure of the resonant tunnelling diode, showing the thickness and material type. 1ML ~0.293nm (left) The AlInGaAs material system viewed with band gap energy against the misfit-strain inducing lattice constant. (right) darkfield TEM image and doping profile.

Figure 1 shows a schematic representation of the RTD layer structure, accompanied by a representative darkfield TEM image of the device active area. The device is grown on semi-insulating Fe-doped InP wafers using a vertical showerhead type MOVPE reactor. To accommodate epitaxial strain conditions, the bulk of the device is lattice-matched $In_{.532}Ga_{.468}As$, whilst the active region consists of a narrow, highly-strained QW $In_{.80}Ga_{.20}As$, sandwiched between 4 atomic monolayer (ML) AlAs barriers. In line with other high-frequency devices, the RTD employs an n-i-n doping scheme, with undoped spacer regions on both ends of the device to prevent the dopant from creating charge-trapped sites or altering the QW confinement levels. For this purpose, asymmetrical spacers were chosen to optimise carrier transit time. Epitaxial layer perfection has been shown to be a critical criteria in the operation of these devices[6], and for this purpose most devices are epitaxially grown using a slow-growth rate, high-vacuum MBE reactor. However, our work replicates earlier successes of high-quality growth using the commercially-scalable MOVPE[7]. We may note that this structure is completely strain-balanced due to the AlAs layers contributing with tensile stress, whereas the QW inducing compressive stress.

The well-known property of mm-wave (and beyond) diodes is their N-shaped I-V-characteristic, which lends itself towards oscillator applications. Since only n+ doping is present, conduction band electrons are the sole contributors to the current. The thin barriers paired with the thin active-device region lead to transit times in the order of ps, with electron dwell times inside the quantum well within fs. However, to exploit this natural potential for oscillation, the RTD requires coupling into a waveguide before being fed into a free-space radiating element.

Figure 2 shows our fabricated slot waveguide, chosen for its design and practical simplicity. Our approach deposits the metal first, followed by a selective wet-etch. The complete details of this dual-pass fabrication technique is discussed elsewhere[5]. This technique allows accurate control of the mesa area whilst maintaining very high quality contacts, using conventional Ti/Au evaporation. After a tapered emitter section and adequate loading (MIM capacitor and stabilisation resistor), the result is a quasi-optical RTD that emits THz radiation out-of-plane. The RTD itself is a circular mesa with fabricated diameters from 3.3µm^2 to 20um^2, with a top contact over the waveguide via the means of a metal air bridge and a bottom contact connected through the n+ layer via a separate electrode. The secondary device formed by the wafer acts as a series resistance, and is a source of loss, however due to the voltage drop across the initial structure, this second device is not expected to go into its negative differential resistance region (NDR).

Downloaded From: https://www.spiedigitallibrary.org/conference-proceedings-of-spie on 8/24/2017 Terms of Use: https://spiedigitallibrary.spie.org/ss/TermsOfUse.aspx

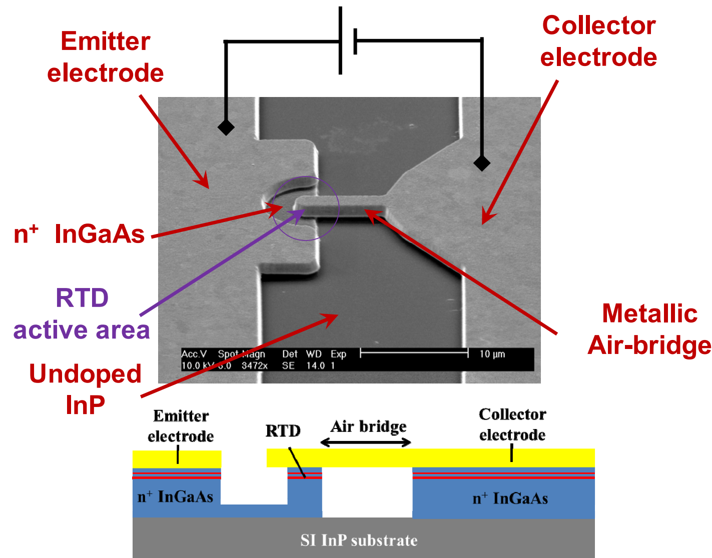

Figure 2. SEM image of a fabricated device showing the electrode layout and the RTD pillar, off-center from a slot waveguide, and connected via an evaporated gold air bridge.

2. TERAHERTZ EMISSION

The device thus described was used to generate THz radiation. In order to measure the output power, we used a commercial room temperature, solid state amplified pyroelectric detector mounted with a TPX window and black coating to remove as many undesirable wavelength components as possible.

In order to measure the THz frequency components, thus confirm that the radiation is indeed in the THz region and not self-heating, we employ a bench-top Fabry-Pérot interferometer, using undoped silicon wafers as the windows and spherical gold mirrors. Since the device emits in the perpendicular plane, 97% of the radiation is absorbed by the InP substrate, therefore a hyperhemispherical Si lens was used to collimate the beam.

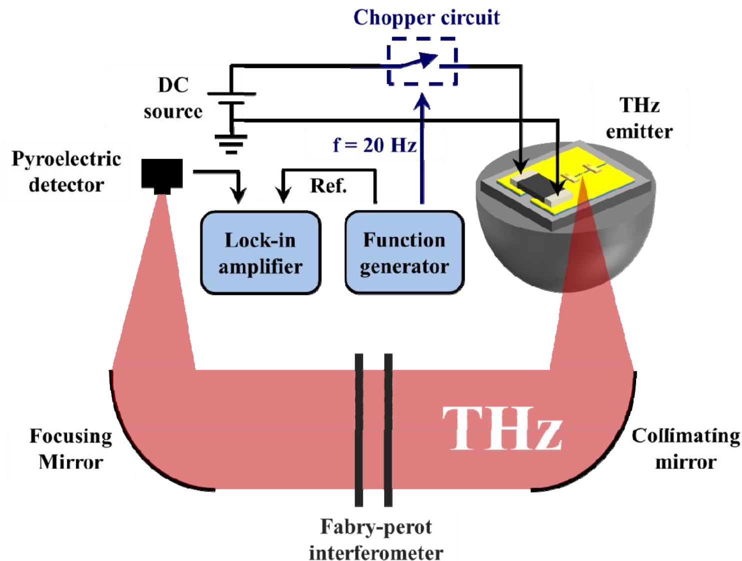

Figure 3. Schematic representation of the experimental apparatus used to measure the THz radiation.

Downloaded From: https://www.spiedigitallibrary.org/conference-proceedings-of-spie on 8/24/2017 Terms of Use: https://spiedigitallibrary.spie.org/ss/TermsOfUse.aspx

In order to improve upon the detector signal to noise ratio, and conform to the detector's requirement for a modulated source, the device is electrically chopped 50% duty at a low frequency of 20Hz (thus operating in a quasi-continuous wave regime) and synchronised to a lock-in amplifier.

In Figure 4, we show the results of the THz measurement. First of all, we compare the loaded and unloaded cases of the RTD device. The loading is purposefully selected to stabilise the small-signal AC oscillation and better match the diode to the waveguide, with R < NDR/2., in this case chosen at 8 ohm. The unloaded DC case can be observed to have a difference from the canonical form of the N-shaped curve. This can be largely attributed to the time-averaged DC instability of the device, for which additional capacitance and larger mesa areas are recommended, going against the requirements of THz components. In the loaded case, most of these oscillations are partially supressed, noting that as a type of chaotic oscillator, RTDs may never be fully stabilised using passive components. Using different lengths of the optical cavity formed by the interferometer Si plates, we obtain a fringe spacing at ~420 µm, with the strongest emission peak at ~353 GHz. We note that the linewidth of the fringes is at the interferometer limit. An instrument with a higher finesse factor is required to study the emission linewidth.

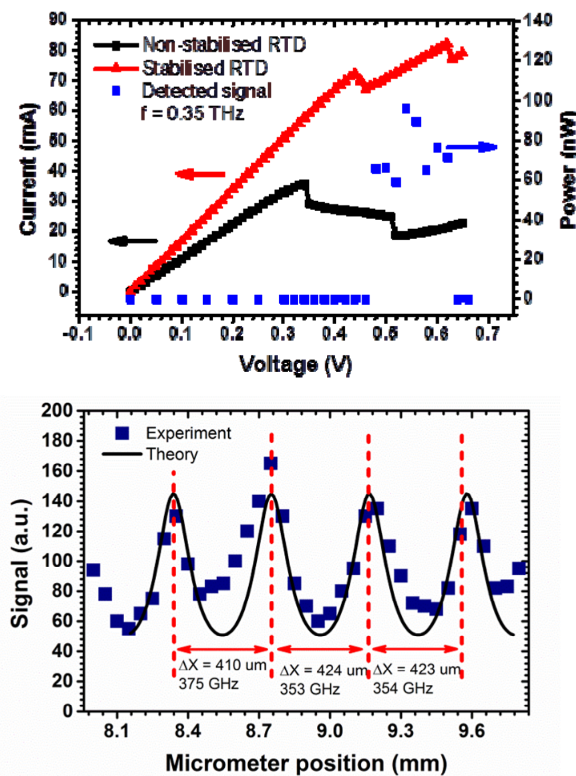

Figure 4. (top) The I-V characteristic and observed THz radiation power. (bottom) Spectrum of the THz radiation measured with the interferometer plotted against a Fabry-Pérot envelope.

3. EPITAXIAL OPTIMISATION

Having replicated the success of these devices as THz emitters, we now proceed to optimise as many aspects of the emitter as possible. An area that is crucial for the operation of such devices has received perhaps insufficient attention in the past 10 years is the epitaxial growth of RTDs. High current density RTD emitters utilise very thin (<2nm), pure AlAs barriers, which create a different set of challenges and unknowns compared to conventional RTDs described in the literature. More importantly, such devices are typically MBE-grown.

Our previous investigation of MOVPE growth[8,9] have demonstrated that high-quality devices can be created using this technique. However, the initial attempt was the result of creating an RTD with stress-compensated epilayers. Based on the assessment criteria highlighted by Sugiyama *et. al.*[7], we have determined that our device is sat above the established

Downloaded From: https://www.spiedigitallibrary.org/conference-proceedings-of-spie on 8/24/2017 Terms of Use: https://spiedigitallibrary.spie.org/ss/TermsOfUse.aspx

trend line. As seen in Figure 5, an ideal device was suggested to have both high peak current densities and a high peak to valley current ratio (PVCR), quantities that come as a natural trade-off as the current density is largely a function of the barrier width, which in turn affects the resonance linewidth, a quantity directly proportional to the PVCR[10].

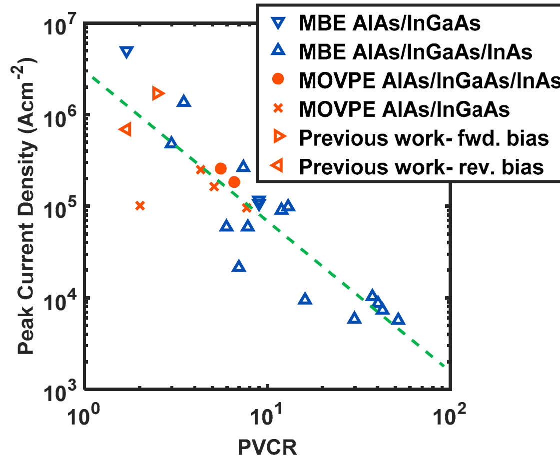

Figure 5. Previous assessment criteria of RTDs, with additions after Sugiyama *et al.*[7] The peak to valley current ratio and current density on a log-log plot. Our high-J RTDs are shown with the left and right-pointing triangles (colour online)

One critique of this assessment criteria is represented by the lack of consideration of the slope of the NDR, a key parameter for impedance matching in practical applications. Furthermore, whilst the PVCR is a good measure of the internal quantum efficiency of the device (the linewidth and amplitude of the electron transmission chance in the resonant state), it offers only a partial indication towards the extractable optical power output.

For this purpose, we have previously discussed a figure of merit that evaluates the overall THz resonator efficiency, based on the ratio between the extractable optical power output against the electrical biasing (chip) power, taken in the middle of the NDR region[11].

In order to optimise the benefit given by a perfect epitaxial growth, we have performed a modelling study[11]. Our findings are summarised in Figure 6, where the height of the graphs shows the resonator efficiency against different QW widths and indium mole fractions. At first sight, a local optimum is reached with a pure InAs QW of 15 ML thickness, with the resonator efficiency dropping towards combinations of long well/high indium content, as the bound levels fall below the Fermi level at resonance.

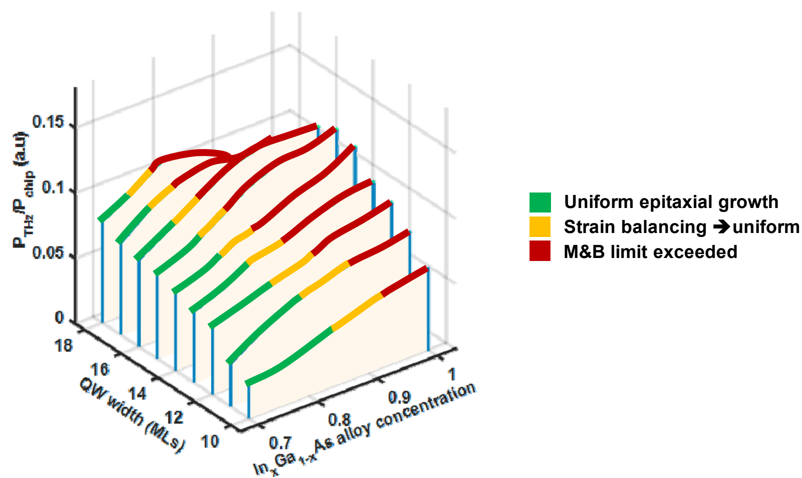

Figure 6. Diagram showing the modelled resonator efficiency with varying QW widths and depths, with 3ML barriers. Colour (online) levels indicate the amount of accumulated stress in the QW, with the red regions exceeding the M&B[12] critical thickness.

Downloaded From: https://www.spiedigitallibrary.org/conference-proceedings-of-spie on 8/24/2017 Terms of Use: https://spiedigitallibrary.spie.org/ss/TermsOfUse.aspx

However, these combinations will result in relaxation of the crystal due to the accumulated stress, ultimately disrupting the barrier interface perfection. Therefore we have calculated the critical thickness of free strained-InGaAs on InP using the worst-case single heterojunction Matthews and Blakeslee model, followed by the contribution of the stress in the opposite direction due to the AlAs barrier growth. Using this limitation, we determine that the optical power can be increased if a similar layer structure is used with thinner barriers. We may, however, note that a thicker well will increase the dwell time of the electrons resulting in a lower cut-off frequency. For the purpose of optimising within the 300-350GHz atmospheric window, this is not an issue however, as GaAs devices, considered inferior to this material system due to the higher electron effective mass, were demonstrated to resonate at 420GHz[13].

4. NON-DESTRUCTIVE CHARACTERISATION

The modelling suggest several candidate structures to be investigated as THz emitters. However, in order to do this in an effective manner, the wafer samples need to be characterised to investigate whether any discrepancies exist, providing feedback to further improve epitaxial perfection. There are several destructive characterisation methods available, of which we could name electrochemical capacitance-voltage (eCV) profiling, secondary ion mass spectroscopy (SIMS), or darkfield TEM imaging. eCV is relatively inexpensive and provides an indication about the doping levels in a sample[9]. Both SIMS and TEM necessarily involve ion milling, a slow process, but provide very good measurements about the sample composition or fine thickness, respectively.

Typical non-destructive characterisation used in the III-V industry involves photoluminescence (PL) spectroscopy and high resolution X-ray diffractometry (HR-XRD). However, PL provides limited information at room temperature as the QW & bulk InGaAs emission overlap strongly. Thus the QW emission peak (Type I transition) remains indistinguishable. However, at low temperature (15 K), significant structural information can be deduced by PL. The problem with this approach was that measuring the precise confined energy level of the resonance remained (ΔE) elusive, as subtle strain-induced band gap profile changes alter its position.

In Figure 7 we show the determination of this ΔE after a “dummy” active region copy buried beneath the n+ contact layer was introduced[14]. The doped QW provides a Type I PL transition whilst the undoped QW provides a Type II transition. This combination of transitions allows ΔE to be unambiguously determined.

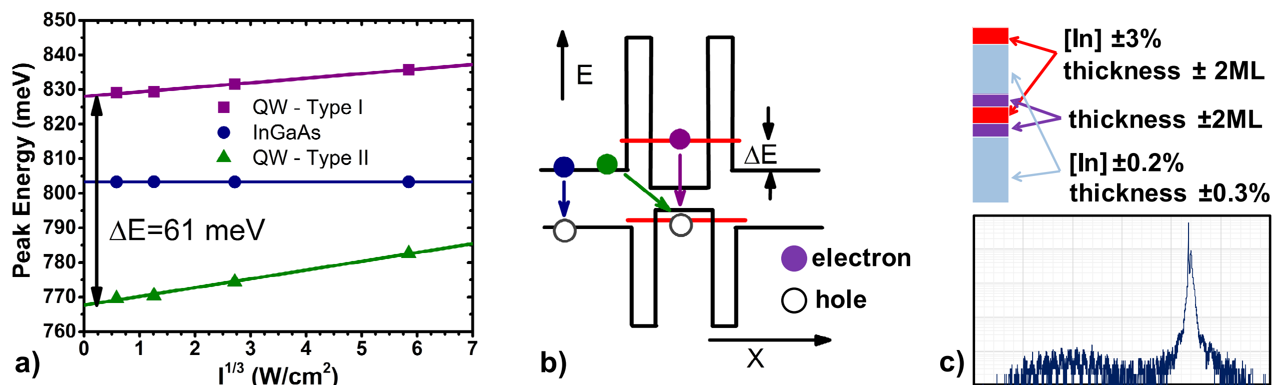

Figure. 7 The non-destructive characterisation scheme based on (a) power-dependent low-temperature photoluminescence spectroscopy given by the (b) possible transitions in the doped and undoped semiconductor case and (c) the contribution of high resolution X-ray diffractometry [004] symmetric rocking curve

Using the Moss-Burstein shift, we have analysed the doping uniformity of our wafers[9]. The linewidth of the PL-emission will provide an indication about the interface accuracy. However, even fitted with the determined ΔE, modelling suggests that there are no unique combinations of structural parameters that achieve this emission. In order to severely narrow down the possibilities, we proceed with HRXRD.

To achieve an adequate signal to noise ratio on a 2θ-ω symmetric (004) rocking curve, we have used a Bruker D8 on the maximum machine setting of angular resolution, a 0D detector set with a suitably high integration time. The X-ray source accelerates 40kV generating a $CuK_{\alpha 1}$ wavelength filtered using a (022) Ge monochromator. To increase the observable Pendellösung fringe spacing, beam slits were used on both incident and diffracted beam.

Downloaded From: https://www.spiedigitallibrary.org/conference-proceedings-of-spie on 8/24/2017 Terms of Use: https://spiedigitallibrary.spie.org/ss/TermsOfUse.aspx

A simplified layer structure was simulated (Figure 7c). As a first step to improve the model fit to the data, a process of linking the mole fraction and relative thickness of various layers was employed. For example any unwanted growth rate difference or compositional variations will be replicated throughout the structure. All LM-InGaAs will be slightly tensile or compressive. We do not expect different alloys to be deposited at different positions in the structure. Once the fit can no longer be adequately improved manually, the layers are decoupled and the algorithms available in the XRD modelling software are deployed in stages to optimise the residual value. The result of a sensitivity analysis is shown. HRXRD is not sensitive to very fine barrier thickness changes, which besets a limitation of the non-destructive method. A combined HRXRD & PL paper will be presented at a later date.

5. CONCLUSION

We have described a quasi-optical RTD emitter using a tapered slot antenna. Its spectral characteristics are shown. We identify key areas which need to be addressed for the improvement of this device. As a first order, we use a figure of merit based on measurements from our own fabricated RTDs, and compare this with other assessment criteria available in the literature. This can then be used as a structural design aid to maximize THz radiation output. The practicality of manufacturing this device has been mentioned in terms of strain relaxation and the formation of misfit dislocations and suggest directions for such manufacturable wafers.

We have reported on the combined use of LT-PL and HRXRD characterisation as a rapid, non-destructive tools in order to monitor the growth quality. We remind about the usage of PL characterisation to measure the absolute doping concentration of the highly doped emitter/collector and contact layers, and identifying key device components from the emission linewidths. The RTD structure with a 'dummy' RTD buried in the InGaAs buffer layer allows us to monitor the structural composition in greater detail, with advantages to both optical techniques. This characterisation method allows description of the layer structure with a high level of accuracy, with the exception of the AlAs barrier thickness

REFERENCES

[1] T. Mukai., M. Kawamura., T. Takada., T. Nagatsuma., "1.5-Gbps wireless transmission using resonant tunneling diodes at 300 GHz," Tech. Dig. Opt. Terahertz Sci. Technol. 2011 Meet., MF42, Santa Barbara (2011).

[2] Maekawa, T., Kanaya, H., Suzuki, S.., Asada, M., "Oscillation up to 1.92 THz in resonant tunneling diode by reduced conduction loss," Appl. Phys. Express **9**(2), 24101 (2016).

[3] Nagatsuma, T., Nishii, H.., Ikeo, T., "Terahertz imaging based on optical coherence tomography \[Invited\]," Photon. Res. **2**(4), B64--B69, OSA (2014).

[4] Cooper, K. B., Dengler, R. J., Llombart, N., Talukder, A., Panangadan, A. V., Peay, C. S., Mehdi, I.., Siegel, P. H., "Fast high-resolution terahertz radar imaging at 25 meters," Terahertz Physics, Devices, Syst. IV Adv. Appl. Ind. Def. **7671**, M. Anwar, N. K. Dhar, and T. W. Crowe, Eds., 76710Y (2010).

[5] Jacobs, K. J. P., Stevens, B. J., Wada, O., Mukai, T., Ohnishi, D.., Hogg, R. A., "A Dual-Pass High Current Density Resonant Tunneling Diode for Terahertz Wave Applications," IEEE Electron Device Lett. **36**(12), 1295–1298 (2015).

[6] Roblin, P., Potter, R. C.., Fathimulla, A., "Interface roughness scattering in AlAs/InGaAs resonant tunneling diodes with an InAs subwell," J. Appl. Phys. **79**(5), 2502 (1996).

[7] Sugiyama, H., Teranishi, A., Suzuki, S.., Asada, M., "Structural and electrical transport properties of MOVPE-grown pseudomorphic AlAs/InGaAs/InAs resonant tunneling diodes on InP substrates," Jpn. J. Appl. Phys. **53**(3), 31202 (2014).

[8] Jacobs, K. J. P., "Development of Resonant Tunnelling Diode Terahertz Emitter," The University of Sheffield (2015).

[9] Jacobs, K. J. P., Stevens, B. J., Mukai, T., Ohnishi, D.., Hogg, R. A., "Non-destructive mapping of doping and structural composition of MOVPE-grown high current density resonant tunnelling diodes through photoluminescence spectroscopy," J. Cryst. Growth **418**, 102–110, Sheffield (2015).

[10] García-Calderón, G., "Tunneling in Semiconductor Resonant Structures," [Physics of Low-Dimensional Semiconductor Structures], P. Butcher and et. al., Eds., Plenum Press, New York, 267–297 (1993).

[11] Baba, R., Stevens, B. J., Mukai, T.., Hogg, R. A., "Optimization of the epitaxial design of high current density resonant tunneling diodes for terahertz emitters," Proc. SPIE 9755, Quantum Sens. Nano Electron. Photonics XIII, 97552W (13 Febr. 2016), M. Razeghi, Ed., 97552W (2016).

Downloaded From: https://www.spiedigitallibrary.org/conference-proceedings-of-spie on 8/24/2017 Terms of Use: https://spiedigitallibrary.spie.org/ss/TermsOfUse.aspx

[12] Matthews, J. W.., Blakeslee, A. E., "Defects in epitaxial multilayers," J. Cryst. Growth **27**, 118–125 (1974).
[13] Brown, E. R., Sollner, T. C. L. G., Parker, C. D., Goodhue, W. D.., Chen, C. L., "Oscillations up to 420 GHz in GaAs/AlAs resonant tunneling diodes," Appl. Phys. Lett. **55**, 1777–1779 (1989).
[14] Jacobs, K. J. P., Baba, R., Stevens, B. J., Mukai, T., Ohnishi, D.., Hogg, R. A., "Characterisation of high current density resonant tunneling diodes for THz emission using photoluminescence spectroscopy," 15 March 2016, 97580L.

Downloaded From: https://www.spiedigitallibrary.org/conference-proceedings-of-spie on 8/24/2017 Terms of Use: https://spiedigitallibrary.spie.org/ss/TermsOfUse.aspx